

 Open access • Journal Article • DOI:10.1364/OL.37.000975

## **Design of a subnanometer resolution beam position monitor for dielectric laser accelerators. — Source link**

Ken Soong, Robert L. Byer

**Institutions:** Stanford University

**Published on:** 01 Mar 2012 - Optics Letters (Optical Society of America)

**Topics:** Particle beam and Particle accelerator

Related papers:

- [Design of a Subnanometer Resolution Beam Position Monitor for Dielectric Laser Accelerators](#)
- [Dielectric laser accelerators](#)
- [Proposed few-optical cycle laser-driven particle accelerator structure](#)
- [Electromagnetic forces in the vacuum region of laser-driven layered grating structures](#)
- [Demonstration of electron acceleration in a laser-driven dielectric microstructure](#)

Share this paper:    

View more about this paper here: <https://typeset.io/papers/design-of-a-subnanometer-resolution-beam-position-monitor-3oz5i9uyd0>

# Design of a sub-nanometer resolution beam position monitor for dielectric laser accelerators

Ken Soong\*, Robert L. Byer

*Department of Applied Physics, Stanford University, Stanford, CA 94305, USA*

*\*Corresponding author: KenSoong@SLAC.Stanford.edu*

Compiled March 1, 2013

We present a new concept for a beam position monitor with the unique ability to map particle beam position to a measurable wavelength. Coupled with an optical spectrograph, this beam position monitor is capable of sub-nanometer resolution. We describe one possible design, and through finite element frequency domain simulations, we show a resolution of 0.7 nanometers. Due to its high precision and ultra-compact form factor, this device is ideal for future x-ray sources and laser-driven particle accelerators “on-a-chip”.

Rapid progress in the development of laser technology and in the sophistication of photonic devices has enabled the realization of the first laser-powered particle accelerators “on-a-chip” [1, 2]. These devices are specifically designed to take advantage of the mass-production techniques of the computer chip industry and offer a far less expensive and far more compact way to build the particle accelerators that will power future generations of cancer treatment machines and ultra-compact monochromatic x-ray sources [3]. Compared to their traditional microwave-powered counterparts, laser-powered accelerators are constructed using dielectrics and semiconductors rather than metals, and have a four order of magnitude reduction in wavelength. Since the accelerating channel in laser-powered accelerators typically have dimensions in the one micron range, the ability to precisely control particle position within these structures will be critical for operation. A number of beam deflection and focusing schemes have been devised [4, 5], but without the ability to measure the position of the particle beam to nanometer-accuracy these schemes will be extremely difficult to implement.

The conventional “beam position monitor” (BPM) exploits the amplitude-dependent coupling of charged particle beams to TM<sub>110</sub> modes of a resonator, encoding position information in the amplitude and phase of the signal. These BPMs typically have a resolution of one micron [6]. However, if heroic measures are taken to control noise in the processing electronics, a BPM resolution on the order of ten nanometers can be achieved [7]. Beam position monitors based on Smith-Purcell radiation from periodic structures have also been proposed [8], which like their conventional counterpart encode position information in a signal amplitude. These Smith-Purcell based BPMs are similarly noise-limited to a resolution on the order of ten nanometers [9].

We present a new concept for a BPM which has the unique ability to map beam position to a measurable wavelength. This novel BPM is capable in principle of resolutions below one nanometer when used in conjunction with an optical spectrograph. Additionally, this

technique avoids the usual saturation problems encountered with large beam position offsets or large variations in beam current, which tend to limit resolution and dynamic range in conventional BPMs.

Our proposed sub-nanometer resolution BPM design is based largely on the principles of the dielectric grating accelerator. At its core, the proposed BPM structure consists of a pair of opposing gratings whose periodicity is a function of position. In the simplest case, consider a structure comprised of a uniform grating of periodicity  $\lambda_g$  and a second identical grating placed above the first, with the teeth facing each other and a finite gap between the two, as shown in Fig. 1. For clarity, we define the axis of separation as the  $y$ -axis and the axis of periodicity as the  $x$ -axis. This structure has been shown to generate an electric field in the gap region capable of accelerating electrons along  $x$  when driven with a planewave as shown in Fig. 1b [4].

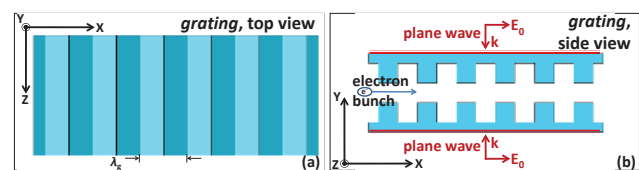


Fig. 1. The dielectric grating accelerator as view from the top (a) and the side (b).

By reciprocity, we expect that an electron bunch traversing an unpowered structure will decelerate and radiate at a wavelength of  $\lambda_g$ . This radiation will be directed symmetrically in the  $+y$  and  $-y$  direction, and can be collected by detectors positioned on either face of the structure. In this case, we have a trivial BPM capable of indicating whether or not the electron bunch is passing through the grating structure. We can add additional functionality to this device by varying the grating period as a function of  $z$ . Fig. 2 shows one such implementation, which we will dub the “clam shell” BPM. The teeth of this grating structure is designed such that any line-out at a fixed  $z$ -location will appear as a uniform periodic

binary grating. This structure can be described geometrically by the coordinates of the  $n$ th tooth in the grating. For any given wavelength,  $\lambda_g$ , the  $n$ th grating tooth begins at  $x_{n,0} = (n-1/4)\lambda_g$  and ends at  $x_{n,1} = (n+1/4)\lambda_g$ . For a design that varies continuously from  $\lambda_{g,1}$  to  $\lambda_{g,2}$  over a distance of  $L$ , the theoretical sensitivity is given by  $L/(\lambda_{g,2} - \lambda_{g,1})$ . In the example shown in Fig. 2, the grating period varies from 800 nm to 1600 nm over a distance of 6  $\mu\text{m}$ , corresponding to a sensitivity of  $\frac{7.5 \text{ nm in } z}{1 \text{ nm wavelength}}$ . When used in conjunction with a typical spectrograph, which has a resolution of 0.10 nm, the clam shell BPM is capable of resolving electron bunch position with an accuracy of 0.75 nm.

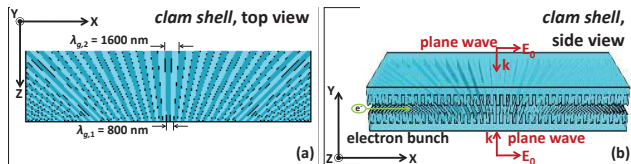


Fig. 2. The top (a) and the side (b) view of the “clam shell” BPM. In this design, the periodicity is constant in  $x$ , but increases continuously in  $z$  from  $\lambda_{g,1}$  to  $\lambda_{g,2}$ .

We simulated the clam shell BPM structure using the commercial finite element frequency domain (FEFD) code HFSS. Although HFSS does not have the capabilities to perform computationally intensive particle-in-cell simulations, which would be the most straight-forward approach to modeling this structure, we can use the principles of reciprocity to obtain all the relevant physical characteristics of this structure. This approach is common with antenna design, where reciprocity asserts that an antenna’s radiation and receiving patterns are identical; or stated more practically, that an antenna functions identically as a transmitter or a receiver. By the same principle, we can use electromagnetic waves to drive our structure, as if it were a transmitter, and then accurately infer the structure’s properties as a receiver.

In the spirit of the reciprocity approach, we simulated the clam shell BPM structure by driving the structure symmetrically from the top and the bottom with planewaves at a discrete set of wavelengths, as depicted in Fig. 2b. The resulting fields from the simulations were then integrated along the  $x$ -direction, taking care to advance the phase of the fields in order to simulate the fields observed by a relativistic electron traveling in  $x$ . The result is a two-dimensional matrix which maps the average accelerating field experienced by a particle as a function of its  $yz$ -location within the structure, as shown in Fig. 3. We found that, for each drive wavelength a single narrow accelerating channel is generated, which by reciprocity implies that the unpowered clam shell BPM has a similarly narrow region where passing electrons will radiate at a particular wavelength.

In addition to the presence of a single narrow accelerating channel, we found that the drive wavelength has a strong effect on the  $z$ -location of this channel, but only a

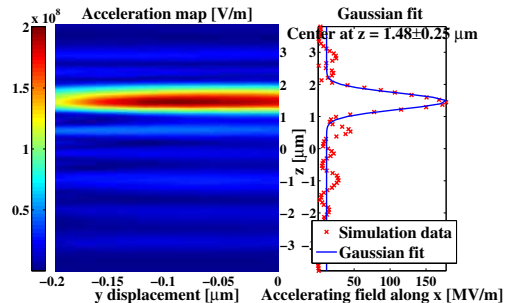


Fig. 3. Simulation results for the “clam shell” BPM driven at  $\lambda_{drive} = 1008 \text{ nm}$ . Left: A map of the accelerating field experienced by a speed of light particle as a function of displacement from the center of the structure. Right: A Gaussian fit to the accelerating field map after flattening along  $y$ .

negligible effect on the  $y$ -location. The linear regression of the drive wavelength against the  $z$ -location of strong acceleration is given explicitly by,

$$z_{acceleration}[\mu\text{m}] = -7.057 \cdot \lambda_{drive}[\mu\text{m}] + 8.770. \quad (1)$$

By the reciprocal nature of this system, we expect that an electron bunch traversing the unpowered clam shell BPM structure will decelerate and radiate at a wavelength unique to the  $z$ -coordinate of the electron bunch. The explicit formula for the radiated wavelength as a function of the  $z$ -coordinate of the electron bunch is given by the inverse of equation (1). Fig. 4 summarizes the relationship between the radiation wavelength and the  $z$ -location of a traversing electron bunch, as determined by the Gaussian fit shown in Fig. 3, with the error bars in the plot representing the width of the Gaussian.

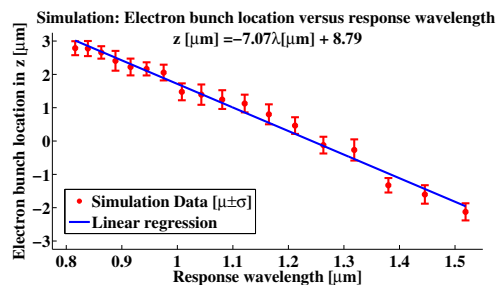


Fig. 4. Simulation of the electron bunch  $z$ -location versus the “clam shell” BPM response wavelength. The markers define the center of the excitation channel as determined by a Gaussian fit to the simulation data, whereas the error bars represent the width of the Gaussian fit.

Given the input power and the resulting electric fields in the accelerating channel, we calculated the expected photon yield from the clam shell BPM structure using an analogy to circuits and Ohm’s law; a common practice in radio-frequency structure design. The average shunt

impedance of the structure was calculated to be,

$$Z_s[\Omega] = \frac{(\int_0^d E_x dl)^2}{P} = 300 \cdot (d[\text{mm}])^2, \quad (2)$$

where  $P$  is the input power and  $d$  is the length of the BPM structure measured in millimeters. Using the shunt impedance, we estimated the photon yield for an electron bunch traversing the unpowered BPM structure to be,

$$N(Q, d, \tau) = 1.85 \times 10^6 \cdot \frac{(Q[\text{fC}] \cdot d[\text{mm}])^2}{\tau[\text{fs}]}, \quad (3)$$

where  $Q$  is the bunch charge measured in femtocoulombs,  $d$  is length of the BPM structure measured in millimeters, and  $\tau$  is the bunch length measured in femtoseconds, assuming  $\tau \ll \frac{\lambda_g}{c}$ . For the application of a laser-driven dielectric accelerator, where  $Q = 10$  fC and  $\tau = 0.1$  fs, and with a 0.2 mm BPM structure, the per bunch photon yield at  $z = 0$  is  $N \approx 7.5 \times 10^7$  photons.

By performing a least-squares Gaussian fit to the radiation spectrum, it is possible to precisely deduce the location of the passing electron bunch, as illustrated in Fig. 5. With the above mentioned beam parameters, a 20 nm spot size electron bunch, and an InGaAs detector array with a NEP on the order of  $30 \frac{\text{fW}}{\sqrt{\text{Hz}}}$  at an operating frequency bandwidth of 10 kHz, we estimate the BPM resolution to be 1.7 nm. However, if the length of the BPM is increased then the resolution of the BPM is improved through two effects: the increase in the radiated power as described by equation (3), and the reduction of the radiation bandwidth as described by the relation [8]:  $\Delta\lambda \propto \frac{\lambda}{d}$ , where  $\lambda$  is the radiation wavelength. With a BPM structure length of 1 mm, the resolution approaches 0.75 nm.

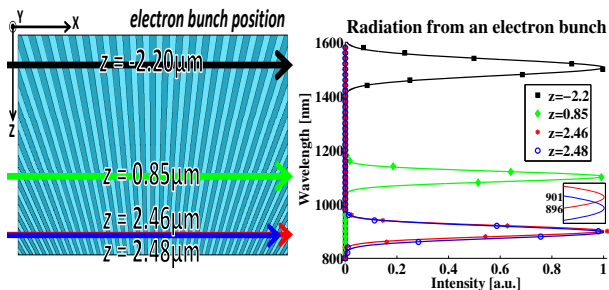


Fig. 5. The predicted normalized radiation spectrum from an electron bunch traversing the “clam shell” BPM at four different  $z$  displacements. The markers on the plot (right) represent simulation data, whereas the solid lines depict a Gaussian fit to the simulation data. The inset highlights the distinct radiation spectrum generated by two closely separated bunches.

In the case where the electron beam traverses the clam shell BPM with a non-zero  $z$ -component of velocity, we expect a chirped output signal. This chirped response will manifest as a broadening of the radiation spectrum, with the Gaussian center of the spectrum representing

the average beam location in  $z$ . The trajectory of the electron beam can be deduced from the bandwidth of the radiation signal. However, the position resolution of the BPM will be reduced by such bandwidth broadening.

The output angle of the emitted photons is given by the synchronicity condition,

$$n \frac{\lambda}{\lambda_g} = \left( \frac{1}{\beta} - \cos \theta \right), \quad (4)$$

where  $n$  is the order of the radiation,  $\beta$  is the ratio of the electron velocity to the speed of light, and  $\theta$  is the angle between the direction of the electron motion and the direction of radiation in the  $xy$ -plane. For the clam shell BPM structure where  $\lambda = \lambda_g$ ,  $n = 1$ , and  $\beta \approx 1$ , we expect to find the strongest radiation at  $\theta = 90^\circ$ , with an angular spread  $\Delta\theta = \frac{n}{\lambda_g \sin \theta} \Delta\lambda = 0.02^\circ$ . Additionally, due to the radiation mechanism, the radiation will be polarized with the electric field in the  $x$ -direction.

We have described a design for a sub-nanometer resolution particle beam position monitor. Through simulations, we have shown a structure design which exhibits a linear relationship between the radiated wavelength and the electron bunch position. Although we described the specific case of an electron beam in this paper, the concepts are general and apply to all charged particle beams. Based on these results, this extremely small form factor BPM is well-suited for future generation x-ray laser sources, as well as future particle colliders.

The author would like to thank E.R. Colby, R.J. England, C. McGuinness, E.A. Peralta, and the E-163 group for their useful discussions. This work is supported by DOE contract DE-AC02-76SF00515 and DE-FG06-97ER41276 and the Stanford Graduate Fellowship.

## References

1. C. McGuinness, E. Colby and R.L. Byer, *J. Modern Optics* **56** (18-19), p.2142 (2009).
2. E.A. Peralta, R.L. Byer, E. Colby, R.J. England, C. McGuinness, and K. Soong, *Proceedings of the 2011 Particle Accelerator Conference*, pp. 280 (2011).
3. T. Plettner, R.L. Byer, *Phys. Rev. STAB* **11**, 030704 (2008).
4. T. Plettner, R.L. Byer, and B. Montazeri, *J. Modern Optics* **58** (17), p.1518 (2011).
5. K. Soong, E. A. Peralta, R. L. Byer, and E. Colby, SLAC Report No. SLAC-PUB-14426 (2011).
6. R. Lill, W. Norum, L. Morrison, N. Sereno, G. Waldschmidt, D. Walters, S. Smith, and T. Straumann, *Proceedings of the 2007 Particle Accelerator Conference*, pp. 4366 (2007).
7. Y. Inoue, H. Hayano, Y. Honda, T. Takatomi, T. Tauchi, J. Urakawa, S. Komamiya, T. Nakamura, T. Sanuki, E. Kim, S. Shin, and V. Vogel, *Phys. Rev. STAB* **11**, 062801 (2008).
8. S.E. Korbly, A.S. Kesar, J.R. Sirigiri, and R.J. Temkin, *Phys. Rev. Lett.* **94**, 054803 (2005).
9. S. Banna, L. Ludwig, and L. Schachter, *Nucl. Instrum. Methods Phys. Res. A* **555**, 101 (2005).

## Informational Fourth Page

### References

1. C. McGuinness, E. Colby and R.L. Byer, "Accelerating electrons with lasers and photonic crystals," *J. Modern Optics* **56** (18-19), p.2142-2147 (2009).  
[http://www.stanford.edu/~rlbyer/PublishedArticles/2009/JMO\\_PQE\\_McGuinness.pdf](http://www.stanford.edu/~rlbyer/PublishedArticles/2009/JMO_PQE_McGuinness.pdf)
2. E.A. Peralta, R.L. Byer, E. Colby, R.J. England, C. McGuinness, and K. Soong, *Proceedings of the 2011 Particle Accelerator Conference*, pp. 280 (2011).  
<http://www.c-ad.bnl.gov/pac2011/proceedings/papers/mop096.pdf>
3. T. Plettner, R.L. Byer, "Proposed dielectric-based microstructure laser-driven undulator," *Phys. Rev. STAB* **11**, 030704 (2008).  
[http://www.stanford.edu/~rlbyer/PDF\\_AllPubs/2008/432.pdf](http://www.stanford.edu/~rlbyer/PDF_AllPubs/2008/432.pdf)
4. T. Plettner, R.L. Byer, and B. Montazeri, "Electromagnetic forces in the vacuum region of laser-driven layered grating structures," *J. Modern Optics* **58** (17), p.1518-1528 (2011).  
<http://www.tandfonline.com/doi/abs/10.1080/09500340.2011.611914>
5. K. Soong, E. A. Peralta, R. L. Byer, and E. Colby, "Simulation Studies of the Dielectric Grating as an Accelerating and Focusing Structure," SLAC Report No. SLAC-PUB-14426 (2011).  
<http://slac.stanford.edu/pubs/slacpubs/14250/slac-pub-14426.pdf>
6. R. Lill, W. Norum, L. Morrison, N. Sereno, G. Waldschmidt, D. Walters, S. Smith, and T. Straumann, "Design and performance of the LCLS cavity BPM system," in *Proceedings of the 2007 Particle Accelerator Conference*, pp. 4366-4368 (2007).  
<http://accelconf.web.cern.ch/AccelConf/p07/PAPERS/FRPMN111.PDF>
7. Y. Inoue, H. Hayano, Y. Honda, T. Takatomi, T. Tauchi, J. Urakawa, S. Komamiya, T. Nakamura, T. Sanuki, E. Kim, S. Shin, and V. Vogel, "Development of a high-resolution cavity-beam position monitor," *Phys. Rev. STAB* **11**, 062801-062813 (2008).  
<http://prst-ab.aps.org/pdf/PRSTAB/v11/i6/e062801>
8. S.E. Korbly, A.S. Kesar, J.R. Sirigiri, and R.J. Temkin, "Observation of Frequency-Locked Coherent Terahertz Smith-Purcell Radiation," *Phys. Rev. Lett.* **94**, 054803 (2005).  
<http://prl.aps.org/abstract/PRL/v94/i5/e054803>
9. S. Banna, L. Ludwig, and L. Schachter, "Wake-field in an array of metallic posts: Possible application for beam position monitoring," *Nucl. Instrum. Methods Phys. Res. A* **555**, 101 (2005).  
<http://www.sciencedirect.com/science/article/pii/S0168900205018267>